

Limits on intrinsic charm from neutrino fluxes at IceCube

Maria Vittoria Garzelli,^a Sergey Ostapchenko^a and Günter Sigl^{a,*}

^a*Universität Hamburg, II. Institute for Theoretical Physics,*

Luruper Chaussee 149, 22761 Hamburg, Germany

E-mail: maria.vittoria.garzelli@desy.de, sergey.ostapchenko@desy.de,
guenter.sigl@desy.de

We derive limits on the intrinsic charm (IC) content of the proton, considering various theoretical models for IC and using as a basis the experimental upper limit on the prompt neutrino flux reported by the IceCube collaboration in their analysis of throughgoing muon tracks from the Northern Hemisphere. Our upper limit on the IC follows from the condition that the total prompt neutrino flux comprising the contributions from both the perturbative QCD heavy-flavour production and the process of freeing and hadronizing IC saturates the IceCube limit.

*The European Physical Society Conference on High Energy Physics (EPS-HEP2023)
21-25 August 2023
Hamburg, Germany*

*Speaker

1. Basics: Calculation of Atmospheric Lepton Fluxes and QCD input

Atmospheric lepton fluxes are usually computed from so-called cascade equations which contain all relevant interactions in the atmosphere. There is a critical energy above which hadron interactions dominate over decay. For charged pions it is about 20 GeV which is relevant for the conventional neutrino flux, whereas for charmed hadrons it is much higher, about 10^7 GeV, which gives rise to the prompt neutrino flux with harder spectrum, compared to the conventional one.

Basic ingredients of the computation of prompt neutrino fluxes are perturbative QCD (pQCD) differential cross sections for single-inclusive charmed-hadron production. The latter depend on parton distribution functions (PDFs) and fragmentation functions (FFs), which in turn depend on the factorization scale μ_f . The PDFs also depend on the longitudinal momentum fraction x of the parton in the initial-state hadron and the FFs on the momentum fraction z inherited by the final-state hadron from the parton. The dependence on μ_f can be treated perturbatively, whereas the x and z dependences contain non-perturbative effects. The theoretical predictions for the partonic cross sections depend on charm-quark (pole) mass m_c , μ_f and the renormalization scale μ_r , and x and z . These ingredients enter the factorization formula

$$d\sigma_{pp \rightarrow D+X} = \sum_{i,j} \text{PDF}(x_i, \mu_f) \text{PDF}(x_j, \mu_f) \otimes d\hat{\sigma}_{ij \rightarrow cX}(x_i, x_j, \mu_f, \mu_r, m_c, z) \otimes \text{FF}_{c \rightarrow D}(z, \mu_f).$$

Theoretical differential cross sections are known to next-to-leading order (NLO), but not yet to next-to-next-to-leading order (NNLO), whereas total cross sections σ for the hadroproduction of an heavy-quark pair are known to NNLO. We note that the present theoretical uncertainties on the single-inclusive D -meson production cross sections are typically larger than the experimental ones. These uncertainties can be reduced, however, by taking ratios of suitable cross sections, such as at different center-of-mass (COM) energies or at different rapidities and the same COM energy. These ratios in comparison with LHCb data have been used to constrain the low- x gluon and sea quark distributions in some PDF sets, in particular the PROSA PDFs [1] and some version [2] of the NNPDF PDFs [3]. Other PDF sets, not including this information, but also used in this contribution, are ABMP16 [4] and CT14 [5].

2. Alternative Method for Z-moment Computation

Following Ref. [6], we introduce an alternative method for the computation of the prompt neutrino flux. There it was shown that one can write down the prompt muon neutrino spectrum as

$$I_{\nu_\mu(\text{prompt})}(E_\nu) \simeq \frac{I_p(E_\nu)}{1 - Z_{p\text{-air}}^p(E_\nu, \gamma_p)} Z_{p\text{-air}}^{\nu_\mu(\text{prompt})}(E_\nu, \gamma_p), \quad (1)$$

where the Z -moment $Z_{p\text{-air}}^X(E_X, \gamma_p)$ for the production of a secondary particle X in a p -air interaction is defined, up to p regeneration, as the ratio of the flux of X -particles $I_X(E_X)$ at energy E_X to the primary all-nucleon cosmic ray (CR) flux at the same energy, if the latter has a power-law form $I_p(E_p) \propto E^{-\gamma_p}$. Factorization of the proton-to-neutrino Z -moment into proton-to-charm quark moment and fragmentation and decay moments then leads to

$$Z_{p\text{-air}}^{\nu_\mu(\text{prompt})}(E_\nu, \gamma_p) \simeq Z_{p\text{-air}}^c(E_\nu, \gamma_p) \left[\sum_{c, \bar{c}} \sum_{h_c} Z_{c(\bar{c}) \rightarrow h_c}^{\text{fragm}}(\gamma_p) Z_{h_c \rightarrow \nu_\mu}^{\text{dec}}(\gamma_p) \right], \quad (2)$$

where

$$Z_{p\text{-air}}^c(E, \gamma) \simeq \int dx_c x_c^{\gamma-1} \frac{\langle A_{\text{air}} \rangle}{\sigma_{p\text{-air}}^{\text{inel}}(E/x_c)} \frac{d\sigma_{pp}^{c(gg)}(E/x_c, x_c)}{dx_c}, \quad (3)$$

with x_c being the charm energy fraction. The approximation in eq. (3) is justified by the fact that most of the cross-section for c -quark production comes from gg fusion. The factorization allows one to study the uncertainties of the neutrino fluxes in terms of c -quark production. Currently, the dependence of the pQCD cross section for charm production on μ_r and μ_f is the biggest source of uncertainty regarding the perturbative contribution to prompt neutrino fluxes, as can be seen in Fig. 1. Further examples of the moment in eq. (3) computed using as input different PDF sets are shown by the lower set of curves in Fig. 3.

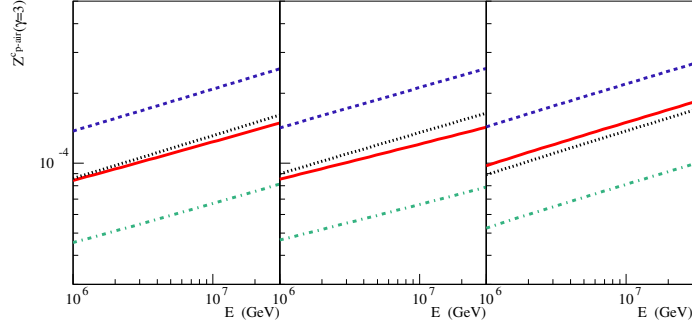


Figure 1: CR spectrum-weighted moments $Z_{p\text{-air}}^c(E, \gamma = 3)$ of c -quark production spectra, calculated using different (μ_r, μ_f) combinations: $(\mu_f, \mu_r) = (1, 1)m_{\perp c}$ (solid), $(\mu_f, \mu_r) = (2, 1)m_{\perp c}$ (dashed), $(\mu_f, \mu_r) = (1, 2)m_{\perp c}$ (dotted-dashed), and $(\mu_f, \mu_r) = (2, 2)m_{\perp c}$ (dotted). The graphs in the left, middle, and right panels are based on gluon PDFs from ABMP16_3_nlo [4], CT14nlo_NF3 [5], and NNPDF31_nlo_pch_as_0118_nf_3 [3] PDF sets, respectively. Taken from Ref. [6].

3. Intrinsic Charm

Intrinsic charm (IC) is represented by proton Fock states of the kind $|uud\bar{c}c\rangle$, $|uud\bar{c}c\bar{c}\rangle$, etc. in which the momentum fraction carried by the c -(anti)quark should be significant, due to the comparable velocities of all quarks [7, 8]. Hadronization of a five-quark Fock state upon interaction with another proton gives rise to processes like $pp \rightarrow \bar{D}^0 + \Lambda_c^+ + X$, $\bar{D}^{*0} + \Lambda_c^+ + X$, etc. . Analogous processes can occur in proton-lepton deep inelastic scattering.

The differential cross section for IC production can be written as [6]

$$\frac{d\sigma_{p\text{-air}}^{c(\text{intr})}(E, x_c)}{dx_c} = w_{\text{intr}}^c \sigma_{p\text{-air}}^{\text{inel}}(E) f_c^{(\text{intr})}(x_c), \quad (4)$$

with w_{intr}^c representing the overall weight of proton Fock states containing IC, that can be decomposed into a product of $w_{\text{intr}}^{c(0)}$ representing the total IC content of the nucleon and $w_{\text{intr}}^{c(\text{frag})}$, i.e. the probability of freeing the IC from the initial bound state and hadronizing it, respectively, and $f_c^{(\text{intr})}(x)$ being the constituent c -quark light-cone momentum fraction distribution, always normalised to unity. For the latter we may consider two models, the corresponding distributions being plotted in Fig. 2. The first one is the original IC model of Brodsky-Hoyer-Peterson-Sakai (BHPS) [7, 8], $f_c^{(\text{intr})}(x) \propto x^2 \left[\frac{1}{3}(1-x)(1+10x+x^2) + 2x(1+x) \ln x \right]$, whereas our second

choice is a Regge ansatz [9, 10] $f_c^{(\text{intr})}(x) \propto x^{-\alpha_\psi} (1-x)^{-\alpha_\psi+2(1-\alpha_N)}$, with α_ψ and α_N being the intercepts for the ψ -meson and nucleon Regge trajectories, respectively.

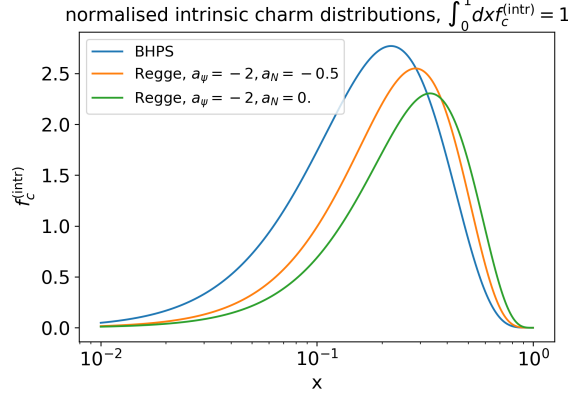


Figure 2: Normalised IC distributions, according to different models.

Using Eq. (4), the Z-moment for the IC contribution follows as

$$Z_{p\text{-air}}^{c(\text{intr})}(\gamma) = Z_{pp}^{c(\text{intr})}(\gamma) = w_{\text{intr}}^c \int dx_c x_c^{\gamma-1} f_c^{(\text{intr})}(x_c). \quad (5)$$

This is neither energy nor target dependent, hence, the corresponding contribution to the neutrino flux follows the primary CR spectrum. In contrast, the prompt component from perturbative charm production is flatter than the primary spectrum, as is obvious from the different slopes of the upper and lower sets of curves in Fig. 3.

While the BHPS model does not provide a prescription for IC hadronization and one often assumes that it proceeds as for the perturbative charm, Regge ansatzs for $f_{D^0}^{(\text{intr})}(x)$ and $f_{\Lambda_c^+}^{(\text{intr})}(x)$ making use of the Regge intercepts exist. They are similar, but not identical to the Regge expression for $f_c^{(\text{intr})}(x)$ (see above), as detailed elsewhere. In fact, it is noteworthy that the hadronisation of constituent c -(anti)quarks may proceed differently, compared to the perturbatively generated ones. For deriving the upper limit on IC, beside the Regge ansatzs with $\alpha_\psi = -2$, $\alpha_n = -0.5$, we also use the model from Hobbs et al. [11], which also comprises the fragmentation of c -(anti)quarks into charmed hadrons.

In turn, to derive a limit on the IC contribution to the prompt neutrino flux, we vary the normalization of the IC contribution w_{intr}^c in such a way that the sum of the perturbative contribution, that we assume to coincide with the pQCD prediction using the PROSA PDFs [1], and the non-perturbative one, saturates the most stringent present IceCube upper limit [12]. In Fig. 4, we show our preliminary results for corresponding constraints, based on the IceCube upper limit for the prompt neutrino flux [12].

4. Conclusions

Recent updates on the prompt neutrino component, based on latest QCD results and experimental data, are important to interpret the measurements of high-energy neutrino fluxes and

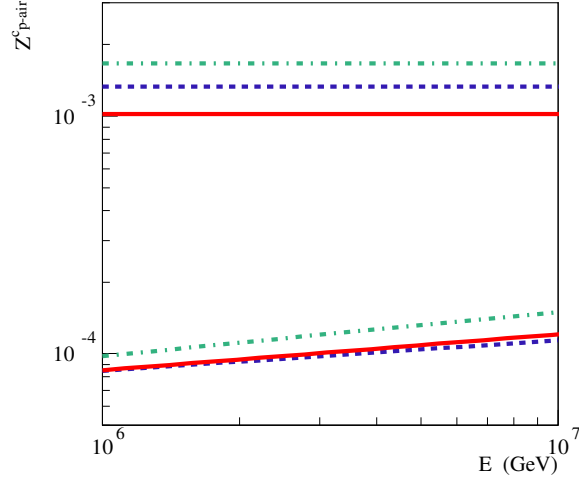


Figure 3: Energy dependence of the CR spectrum-weighted moment, $Z_{p\text{-air}}^c(E, \gamma)$, for perturbative c -quark production in proton-air collisions, calculated using $\gamma = 3$ and employing gluon PDFs from CT14nlo_NF3 [5], PROSA [1], and NNPDF31_nlo_pch_as_0118_nf_3 [3] PDF sets – lower solid, dashed, and dashed-dotted lines, respectively. Shown by the upper solid, dashed, and dashed-dotted lines is the moment $Z_{p\text{-air}}^{c(\text{intr})}$ for the IC contribution, calculated using the BHPS model, the Regge ansatz with $\alpha_N = -0.5$, and with $\alpha_N = 0$, correspondingly, all for $w_{\text{intr}}^c = 0.01$ and $\mu_f = \mu_r = m_{\perp c}$.

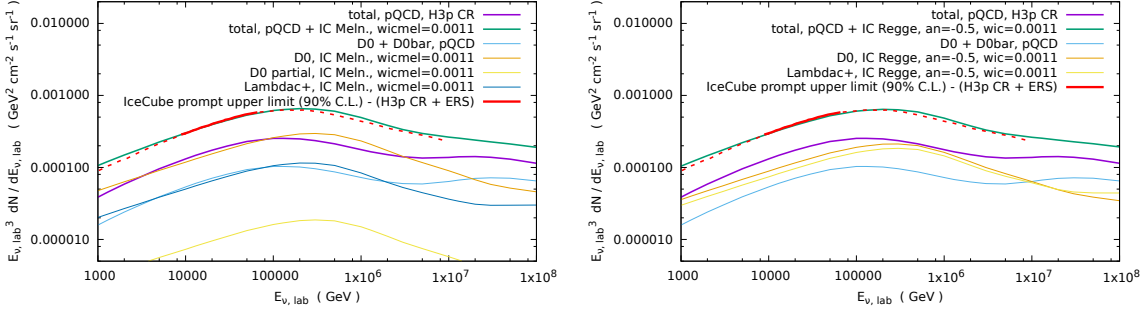


Figure 4: Preliminary upper limits on the IC-induced atmospheric neutrino flux, for the model of Ref. [11], here labelled as “IC Meln”, (left panel) and for the Regge model (right panel), based on IceCube data. The contribution of IC hadronizing in Λ_c^+ and \bar{D}^0 are shown separately.

to disentangle astrophysical neutrinos from atmospheric ones. The deduced uncertainties on the prompt neutrino component are relatively large, up to a factor ≈ 5 , being dominated by pQCD, and for $E_{\nu, \text{LAB}} \gtrsim 10^6$ GeV by the poorly understood CR all-nucleon flux. For neutrinos produced in the atmosphere by interactions of CRs with energies below the “knee”, the prompt flux from IC has a slightly softer spectrum than the prompt flux from perturbative charm production and can thus potentially be disentangled. This allows one to put constraints on IC, based on IceCube data, if the difference in the slopes is sufficiently large. In light of our computations, IceCube results lead to an upper bound on IC normalization of order $w_{\text{intr}}^c \approx 0.001$, rather independent of the IC model.

Acknowledgements

The work of M.V.G. was partially supported by the Bundesministerium für Bildung und Forschung (BMBF), under contract 05H21GUCCA. S.O. acknowledges financial support from Deutsche Forschungsgemeinschaft (project number 465275045). G.S. acknowledges support by BMBF under grant 05A20GU2.

References

- [1] PROSA collaboration, *PROSA PDFs and astrophysical applications*, *Acta Phys. Polon. Supp.* **12** (2019) 885 [1812.02717].
- [2] V. Bertone, R. Gauld and J. Rojo, *Neutrino Telescopes as QCD Microscopes*, *JHEP* **01** (2019) 217 [1808.02034].
- [3] NNPDF collaboration, *Parton distributions from high-precision collider data*, *Eur. Phys. J. C* **77** (2017) 663 [1706.00428].
- [4] S. Alekhin, J. Blümlein and S. Moch, *NLO PDFs from the ABMP16 fit*, *Eur. Phys. J. C* **78** (2018) 477 [1803.07537].
- [5] S. Dulat, T.-J. Hou, J. Gao, M. Guzzi, J. Huston, P. Nadolsky et al., *New parton distribution functions from a global analysis of quantum chromodynamics*, *Phys. Rev. D* **93** (2016) 033006 [1506.07443].
- [6] S. Ostapchenko, M.V. Garzelli and G. Sigl, *On the prompt contribution to the atmospheric neutrino flux*, *Phys. Rev. D* **107** (2023) 023014 [2208.12185].
- [7] S.J. Brodsky, P. Hoyer, C. Peterson and N. Sakai, *The Intrinsic Charm of the Proton*, *Phys. Lett. B* **93** (1980) 451.
- [8] S.J. Brodsky, C. Peterson and N. Sakai, *Intrinsic Heavy Quark States*, *Phys. Rev. D* **23** (1981) 2745.
- [9] A.B. Kaidalov, *$J/\psi c\bar{c}$ production in e^+e^- and hadronic interactions*, *JETP Lett.* **77** (2003) 349 [hep-ph/0301246].
- [10] A.B. Kaidalov and O.I. Piskunova, *INCLUSIVE SPECTRA OF BARYONS IN THE QUARK - GLUON STRINGS MODEL*, *Z. Phys. C* **30** (1986) 145.
- [11] T.J. Hobbs, J.T. Londergan and W. Melnitchouk, *Phenomenology of nonperturbative charm in the nucleon*, *Phys. Rev. D* **89** (2014) 074008 [1311.1578].
- [12] ICECUBE collaboration, *Observation and Characterization of a Cosmic Muon Neutrino Flux from the Northern Hemisphere using six years of IceCube data*, *Astrophys. J.* **833** (2016) 3 [1607.08006].